Metal–support interaction: titania-supported nickel–iron catalysts

J. van de Loosdrecht [a,1], A.M. van der Kraan [b], A.J. van Dillen [a] and J.W. Geus [a]

[a] *Utrecht University, Department of Inorganic Chemistry, Sorbonnelaan 16, 3584 CA Utrecht, The Netherlands*
[b] *Delft University of Technology, Interfacultair Reactor Instituut, Mekelweg 15, 2629 JB Delft, The Netherlands*

Received 1 April 1996; accepted 1 July 1996

The influence of the titania support and metal particle size on the performance of nickel–iron catalysts in the Fischer–Tropsch synthesis has been studied by varying the nickel–iron loading and, consequently, varying the nickel–iron particle size. Low-loaded titania-supported nickel–iron catalysts (2 wt%) turned out to be more selective towards higher hydrocarbons than high-loaded nickel–iron catalysts (20 wt%), which produce much more methane. From temperature-programmed hydrogenation experiments, magnetic measurements and Mössbauer spectroscopy it followed that different types of carbon are present on the catalysts depending on the metal loading. These types of carbon could be related to the selectivity in Fischer–Tropsch synthesis and to the deactivation of the catalysts with time on stream. These differences in catalytic behaviour are most likely due to the presence of TiO_x species on the surface of the active phase, which species decrease the CO and H_2 adsorption properties of the catalyst, but increase the dissociation of CO.

Keywords: Fischer–Tropsch synthesis; nickel–iron; particle size; metal–support interaction

1. Introduction

The activity and selectivity of supported catalysts in Fischer–Tropsch synthesis can be affected by many factors. It has been shown that alloying iron with nickel can increase the CO conversion drastically, whereas the selectivity towards higher hydrocarbons remains the same or decreases slightly [1,2]. Also the deactivation and the carbidization of supported iron catalysts are influenced by the presence of nickel. The effects on activity and selectivity are due to changes in the adsorption of carbon monoxide and hydrogen and to changes in the ability of the active phase to dissociatively adsorb carbon monoxide.

The performance of a catalyst can also be influenced by varying the particle size of the supported active phase [3,4]. The activity of supported cobalt catalysts in Fischer–Tropsch synthesis has been found to depend on the dispersion. However, the selectivity did not change as a function of the metal particle size [3]. Carbon deposition and graphite formation on supported catalysts exposed to carbon containing gas mixtures are more pronounced on large metal particles than on small particles. This difference can affect the catalytic performance and the deactivation of the catalysts with time on stream [4].

In previous research [1,2] it has been shown that the titania support can have a very large effect on the catalytic performance of supported nickel catalysts in the Fischer–Tropsch synthesis. It was shown that depending on the reduction temperature and the nickel loading, which determines the size of the nickel particles, the selectivity towards higher hydrocarbons could increase drastically. Tauster et al. [5,6] denominated the effect of the reduction temperature on titania-supported metal catalysts "strong metal–support interaction" (SMSI). Presently it is generally believed that the changes in the catalytic properties of titania-supported catalysts are caused by the presence of TiO_x ($x < 2$) species on the surface of the active phase [6,7].

Therefore, we will in this study deal with the influence of the titania support and of the metal particle size on the catalytic behaviour of nickel–iron catalysts in the Fischer–Tropsch synthesis by varying the nickel–iron loading and, consequently, varying the nickel–iron particle size.

2. Experimental

Catalyst preparation. Titania-supported nickel–iron catalysts of a Ni/Fe ratio of 1.5 were prepared by deposition–precipitation of bimetallic cyanide complexes [2,8]. After precipitation the catalyst precursors were dried and calcined at 573 K for 3 h. The rate at which the catalyst precursors were heated to 573 K was 3 K/min. The total metal loading was varied between 2 and 20 wt%. A detailed description of the above preparation procedure is published elsewhere [2,8]. The catalysts code xNiFe/support means a supported nickel–iron catalyst of a metal loading of x wt%. In the catalysts a small amount of potassium is present due to the use of $K_3Fe(CN)_6$ in the precipitation method [8]. These amounts are 0.2, 0.1, 0.05 and 0.02 wt% potassium in 20NiFe/TiO_2, 10NiFe/TiO_2, 5NiFe/TiO_2 and 2NiFe/TiO_2, respectively.

[1] Present address: Sastech R&D, PO Box 1, Sasolburg 9570, South Africa.

Fischer–Tropsch synthesis. Fischer–Tropsch synthesis was carried out in a fully automated micro-flow apparatus with a quartz reactor, i.d. 10 mm, operated at atmospheric pressure. The reaction products were analyzed by means of a Perkin Elmer 8700 gas chromatograph equipped with a FID containing a methanizer. A Poropack Q column was used, which was operated between 353 and 473 K. Carbon monoxide, carbon dioxide and hydrocarbons from methane up to heptane were measured. About 350 mg of catalyst was reduced in situ in a 10% hydrogen in helium gas flow of a flow rate of 100 ml/min. During the reduction the temperature was linearly raised from 313 to 673 K at a rate of 1 K/min and subsequently kept constant for 9 h at 673 K. Then the reactor was cooled down to 523 K and a synthesis gas mixture, with $H_2/CO = 2$ and a flow rate of 30 ml/min, was passed through the reactor for 6 h. The syngas concentration in helium was slowly increased up to 100% in 30 min to prevent a sudden and large temperature increase in the catalyst bed due to the exothermic reaction. Schulz–Flory parameters were determined from propane to hexane.

Magnetic measurements. The experiments were executed using a modification of the Weiss-extraction technique as described by Selwood [9]. The apparatus, which has been described elsewhere [2], enabled us to perform in situ magnetization measurements in the temperature range of 295–850 K and at magnetic field strengths up to 0.85 MA m^{-1} (1 MA $m^{-1} = 1.26 \times 10^4$ Oe).

Temperature-programmed hydrogenation (TPH). Temperature-programmed hydrogenation experiments were executed to determine the nature and the amount of carbon species present in the catalysts after Fischer–Tropsch synthesis. To do so, the catalyst was cooled down from the reaction temperature (525 K) to room temperature in a helium gas flow. Next, a 10% hydrogen in helium gas flow was passed through the catalyst bed and the temperature was increased from 300 to 873 K at a rate of 5 K/min. Carbon containing compounds in the gas flow beyond the reactor were measured each minute with a Perkin Elmer 8700 gas chromatograph.

X-ray photoelectron spectroscopy (XPS). X-ray photoelectron spectroscopic measurements were executed with a standard Vacuum Generators MT 500/clam-2 spectrometer using Mg K_α radiation produced by a Mg/Al anode. To calculate the particle sizes from the XPS data, a dispersion analysis program was used, based on a publication of Kuipers [10] and modified by Gijzeman [11].

X-ray diffraction (XRD). X-ray diffraction measurements were carried out with an Enraf Nonius PDS120 X-ray powder diffractometry system using Fe $K_{\alpha 1,2}$ radiation ($\lambda = 1.93735$) to determine the particle sizes of the calcined catalysts. To calculate the particle size from the diffractogram the Scherrer equation was used [12,13].

3. Results and discussion

3.1. Determination of mean particle size

The particle sizes of the cyanide catalyst precursors, the calcined catalysts and the catalysts after reduction as determined from different techniques are represented in table 1. It has been found that the particle size of the cyanide catalyst precursors is much larger than the particle size after calcination and reduction. This larger size can be due to the fact that the cyanide catalyst precursors contain a very large amount of cyanide (CN) ligands. It is also observed that in general, the particle size increases with increasing nickel–iron loading.

3.2. Reduction experiments

The *magnetization* of all catalysts was measured at 673 K, after reduction of the samples for 16 h in 10% H_2 in helium at 673 K (table 2). The magnetization drops at decreasing amounts of nickel–iron, however, not proportional with the metal loading. To clarify the relation between the magnetization and the metal loading we have also calculated the expected magnetization by dividing the magnetization of 20NiFe/TiO_2 by 2, 5 and 10, assuming that when, for instance, the metal loading is decreased by a factor of two the magnetization should

Table 1
The particle size of the cyanide catalyst precursors, the calcined catalysts, and the reduced catalysts as determined by XPS, XRD, oxygen chemisorption and Mössbauer spectroscopy

Catalyst	Particle size (Å)				
	cyanide XPS	calcined XRD	calcined XPS	reduced O_2 chem	reduced Mössbauer
2NiFe/TiO_2	28	–	–	32	< 100
5NiFe/TiO_2	74	–	20	35	–
10NiFe/TiO_2	146	58	40	40	–
20NiFe/TiO_2	202	70	74	74	> 100
2NiFe/Al_2O_3	–	–	60	–	–
20NiFe/Al_2O_3	–	–	80	–	–

Table 2
The measured and expected magnetization of the reduced catalysts, determined at 673 K

Catalyst	M (a.u.)		Deviation (%)
	measured	expected [a]	
20NiFe/TiO_2	7406	7406	–
10NiFe/TiO_2	3438	3703	7
5NiFe/TiO_2	1401	1852	24
2NiFe/TiO_2	321	741	57

[a] The expected magnetization is calculated by dividing the magnetization of 20NiFe/TiO_2 by respectively 2, 5 and 10.

also decrease by a factor of two (table 2). From the data of table 2 it is clear that the lower the metal loading, the larger the difference between the measured magnetization and the calculated magnetization. The larger difference at lower loadings can be caused by a decreasing degree of reduction of the paramagnetic nickel–iron oxidic phase to a ferromagnetic nickel–iron alloy at lower metal loadings.

Mössbauer spectroscopic experiments were executed to study the bulk properties of the iron species present in 2NiFe/TiO_2, 10NiFe/TiO_2 and 20NiFe/TiO_2 after calcination and after reduction. In fig. 1 the Mössbauer spectra of 2NiFe/TiO_2 and 20NiFe/TiO_2 are shown. After calcination both catalysts contain small Fe_2O_3 particles, which do not exhibit a magnetic hyperfine splitting. After reduction the Mössbauer spectrum of 20NiFe/TiO_2 consists mainly of a sextuplet with broad lines due to the presence of Fe(0) in a nickel–iron alloy. Furthermore, a small singlet is present at the center of the spectrum due to a superparamagnetic nickel–iron alloy and a small doublet, which is caused by an Fe(II) base. The Mössbauer spectrum of 2NiFe/TiO_2 after reduction consists mainly of a doublet due to an iron(II) phase and a singlet caused by a superparamagnetic nickel–iron alloy. The fraction of the metal present as an alloy after reduction is 36% for 2NiFe/TiO_2, 79% for 10NiFe/TiO_2, and about 86% for 20NiFe/TiO_2, while the amount of Fe(II) is 64% for 2NiFe/TiO_2, 21% for 10NiFe/TiO_2 and about 14% for 20NiFe/TiO_2 (table 3). The catalyst with a low loading (2 wt%) thus shows a degree of reduction, which is much lower than these of the highly loaded catalysts. This result was also observed with the magnetic measurements described above.

The difference in degree of reduction between 2NiFe/TiO_2 and 20NiFe/TiO_2 can be due to the presence of an interfacial compound between the active metallic phase and the oxidic support, in which iron is present as Fe(II). When even the thickness of the interfacial layer is equal for both catalysts, the ratio of the active components in the not reduced interfacial layer and in the metallic active phase will be much larger for catalyst 2NiFe/TiO_2 than for catalyst 20NiFe/TiO_2.

3.3. Fischer–Tropsch synthesis

The CO conversion is represented as a function of time on stream in fig. 2. The initial CO conversion rises from 15 to 31% with increasing nickel–iron loading from 2 to 20 wt%. However, after 6 h of Fischer–Tropsch synthesis the CO conversion has dropped to about 12% independent of the metal loading. The relative deactivation with time on stream is hence less for catalysts with a low metal loading. These effects related to the nickel–iron loading have also been observed for titania-supported nickel catalysts [1]. The deactivation of the nickel–iron catalysts will be discussed later on.

As we observed that the selectivities of the nickel–iron catalysts towards CO_2, CH_4, C_2 and C_{3+} are almost constant in time, the selectivities have been presented as a function of the metal loadings in figs. 3 and 4. The selectivity towards higher hydrocarbons (C_{3+}) is about 39% for 20NiFe/TiO_2 and 10NiFe/TiO_2 and increases to about 54% for 2NiFe/TiO_2. The CO_2 selectivity

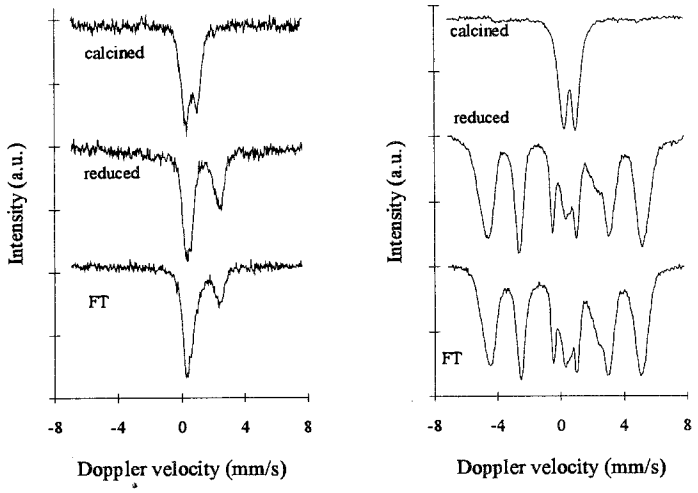

Fig. 1. Mössbauer spectra of 2NiFe/TiO_2 (left) and 20NiFe/TiO_2 (right).

Table 3
Mössbauer data of 2NiFe/TiO_2, 10NiFe/TiO_2 and 20NiFe/TiO_2 after calcination, reduction and Fischer–Tropsch synthesis

Catalyst	IS (mm/s)	QS (mm/s)	HF (kOe)	SC (%)	Compound
2NiFe/TiO_2					
calcined	0.34	0.57	–	26	Fe_2O_3
	0.66	0.74	–	74	Fe_2O_3
reduced	0.26	–	–	36	NiFe alloy superparam.
	1.48	1.81	–	64	Fe(II)
Fischer–Tropsch	0.26	–	–	43	NiFe alloy superparam.
	0.86	0.45	–	14	Fe carbide?
	1.48	1.81	–	43	Fe(II)
10NiFe/TiO_2					
calcined	0.61	0.80	–	100	Fe_2O_3
reduced	0.23	–	–	8	NiFe alloy superparam.
	0.26	–	296	71	NiFe alloy
	1.43	1.72	–	21	Fe(II)
Fischer–Tropsch	0.22	–	–	9	NiFe alloy superparam.
	0.26	–	290	59	NiFe alloy
	1.44	1.87	–	32	Fe(II)
20NiFe/TiO_2					
calcined	0.63	0.78	–	100	Fe_2O_3
reduced	0.26	–	–	6	NiFe alloy superparam.
	0.26	–	306	80	NiFe alloy
	1.45	1.68	–	14	Fe(II)
Fischer–Tropsch	0.23	–	–	7	NiFe alloy superparam.
	0.26	–	295	73	NiFe alloy
	1.42	1.85	–	20	Fe(II)

increases with increasing metal loading, whereas the CH_4 and C_2 selectivities do not depend very much on the metal loading.

The large differences in the C_{3+} and CO_2 selectivities at varying metal loadings can be attributed to several effects. Firstly, a change in particle size as a function of the nickel–iron loading which may lead to the observed differences in selectivities. Secondly, a change in particle size which may modify the influence of the titania support on the performance of the active phase [5,6,14]. To decide about an effect of merely the size of the alloy particles, additionally two alumina-supported nickel–iron catalysts with a nickel–iron loading of 2 and 20 wt% were measured. To assess an effect of the interaction with the titania support a comparison will be made with the results of supported nickel catalysts of a previous study [1,2].

The performance of the alumina-supported nickel–iron catalysts was measured and the production of higher hydrocarbons (C_{3+}) turned out to be 25% for 20NiFe/TiO_2 and 16% for 2NiFe/TiO_2. Although the alloy particle size rises with increasing metal loading for both the titania- and the alumina-supported catalysts (table 1), it follows from the Fischer–Tropsch measurements that the titania-supported catalysts show an increase of the C_{3+} selectivity with decreasing particle size, whereas, the alumina-supported nickel–iron cat-

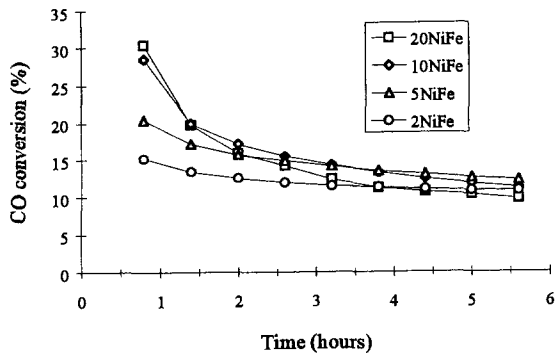

Fig. 2. CO conversion as a function of time on stream during Fischer–Tropsch synthesis at 525 K for 2NiFe/TiO_2, 5NiFe/TiO_2, 10NiFe/TiO_2, and 20NiFe/TiO_2.

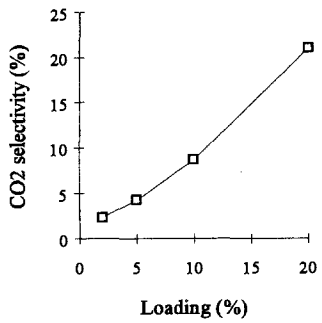

Fig. 3. CO_2 selectivity as a function of the metal loading after 6 h of Fischer–Tropsch synthesis.

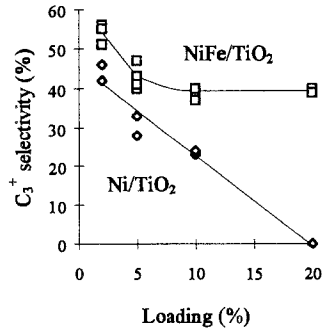

Fig. 4. C_{3+} selectivity as a function of the metal loading for nickel and nickel–iron catalysts after 6 h of Fischer–Tropsch synthesis.

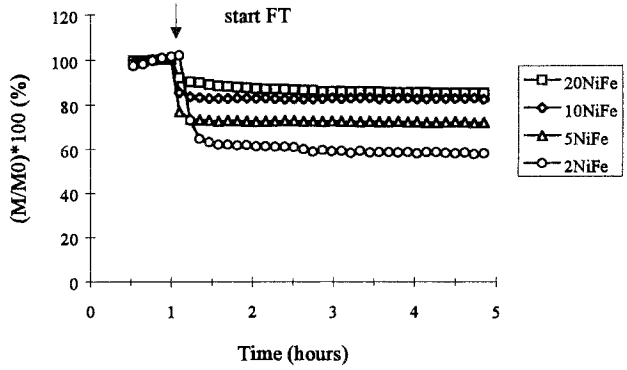

Fig. 5. The magnetization as a function of time during 4 h of Fischer–Tropsch synthesis, for catalysts 2NiFe/TiO_2, 5NiFe/TiO_2, 10NiFe/TiO_2 and 20NiFe/TiO_2.

alysts exhibit a decrease of the production of higher hydrocarbons. Therefore, it is concluded that the changes in the selectivities of the titania-supported nickel–iron catalysts as a function of the metal loading do not essentially depend on the particle size of the active phase.

In fig. 4 the C_{3+} selectivities of different nickel and nickel–iron catalysts are represented together. The 20Ni/TiO_2 catalyst does not produce any C_{3+} hydrocarbons, whereas 20NiFe/TiO_2 has a C_{3+} selectivity of 39%. This difference is due to the presence of iron in the nickel–iron alloy catalyst [2,8]. At decreasing metal loadings both nickel and nickel–iron catalysts produce relatively more higher hydrocarbons. This increase in C_{3+} selectivity of the nickel catalysts with decreasing nickel loading is proven to be caused by partial reduction of TiO_2 to TiO_x species [1,2]. The TiO_x species are in intimate contact with the active metal phase or cover part of the active phase and thus change the CO and H_2 dissociation properties. As the effects observed with the supported nickel catalysts can also influence the catalytic performance of other supported metal catalysts [6] we believe that the increase of the C_{3+} selectivity of the nickel–iron catalysts with decreasing metal loading is also caused by partial reduction of the titania support. The nickel–iron catalysts are more selective towards higher hydrocarbons than the nickel catalysts for all metal loadings. The higher selectivity is most likely due to the different active phase, nickel–iron instead of pure nickel.

3.4. Changes in active phase during Fischer–Tropsch synthesis

To study the behaviour of the catalysts under Fischer–Tropsch conditions magnetic measurements and Mössbauer spectroscopic experiments were performed.

In fig. 5 the changes in the *magnetization* are represented as a function of time during Fischer–Tropsch synthesis. In general the course of the magnetizations is similar for the nickel–iron catalysts with 2, 5, 10, and 20 wt% loading. Initially the magnetization decreases steeply, but after 30 min it reaches a level that remains constant. The observed sharp decrease is probably due to a fast oxidation and/or carbidization of the surface of the nickel–iron alloy, whereas the bulk of the nickel–iron particles remains in the alloyed state. The relative decrease of the magnetization turns out to be higher the lower the metal loading, viz., 15% for 20NiFe/TiO_2 and 42% for 2NiFe/TiO_2. The different drop in magnetization can be explained by a difference in dispersion, which causes a different surface-to-bulk ratio.

Mössbauer spectra were obtained before and after Fischer–Tropsch synthesis for 2NiFe/TiO_2 and 20NiFe/TiO_2 (fig. 1). Before Fischer–Tropsch synthesis the spectrum of 20NiFe/TiO_2 consists of a sextuplet ascribed to a nickel–iron alloy, a singlet due to a superparamagnetic nickel–iron alloy and a doublet caused by an Fe(II) species. After 4 h of Fischer–Tropsch synthesis the spectrum remains almost the same. Only the amount of Fe(II) increases slightly and the hyperfine field of the sextuplet decreases a little, indicating that a small amount of iron is oxidized and is segregated from the nickel–iron alloy [15]. The spectrum of 2NiFe/TiO_2 measured before Fischer–Tropsch synthesis consists of a singlet caused by a superparamagnetic nickel–iron alloy and a doublet connected with the presence of an Fe(II) compound. After Fischer–Tropsch synthesis the spectrum of 2NiFe/TiO_2 contains besides the two species already present before the Fischer–Tropsch synthesis, also a doublet which probably demonstrates the presence of a superparamagnetic iron carbide.

3.5. Deactivation and carbon deposition

To gain more information about the differences in deactivation and catalytic performance of catalysts with a high and a low metal loading, *temperature-programmed hydrogenation* (TPH) experiments were performed. In general, it is found that the carbon present on the low-loaded catalysts (2 and 5 wt%) is more reactive than the carbon present on the high-loaded catalysts (10 and 20 wt%), while the total amount of carbon present

Table 4
The amount of carbon deposited after 6 h of Fischer–Tropsch synthesis

Catalyst	mg carbon/ g catalyst	mg carbon/ g metal	mol carbon/ mol metal
20NiFe/TiO_2	7.7	39	0.18
10NiFe/TiO_2	5.4	54	0.25
5NiFe/TiO_2	6.3	126	0.57
2NiFe/TiO_2	4.6	230	1.0

after 6 h of Fischer–Tropsch synthesis is more or less equal for all catalysts (table 4). However, the amount of carbon related to the amount of metal present on the catalyst decreases with increasing metal loading. Combining this result with the magnetic measurements, it follows that the amount of carbon taken up by the catalyst is related to the decrease of the magnetization during Fischer–Tropsch synthesis. The relation between the amount of carbon and the magnetization also indicates that the decrease of the magnetization is at least for a significant fraction due to carbidization of the surface of the nickel–iron alloy phase.

In fig. 6 the TPH patterns of 20NiFe/TiO_2 and 2NiFe/TiO_2 after 6 h of Fischer–Tropsch synthesis are compared with those of 20Ni/TiO_2 and 2Ni/TiO_2, which already have been published elsewhere [1,2]. The TPH profiles of the high-loaded catalysts are significantly different. The 20Ni/TiO_2 catalyst, which produces only methane during Fischer–Tropsch synthesis, shows only one, very active, type of carbon (α'-carbon [16]), which is hydrogenated between 400 and 500 K. By contrast the 20NiFe/TiO_2 catalyst shows a very small amount of α'-carbon, but a high amount of carbon hydrogenated between 500 and 650 K (α-carbon), and additionally a small amount of carbon which is hydrogenated above 650 K (β-carbon) [16]. This last catalyst produces, besides a relatively small amount of methane, mainly higher hydrocarbons (C_{3+}). Obviously, α'-carbon is involved in the reaction to methane and one of the other types of carbon takes part in the formation of the higher hydrocarbons. Furthermore, the 20Ni/TiO_2 catalyst did not show deactivation with time on stream, whereas the 20NiFe/TiO_2 catalyst does. So it follows that α'-carbon does not cause deactivation and, consequently, α- and/or β-carbon has to be responsible for the deactivation of 20NiFe/TiO_2.

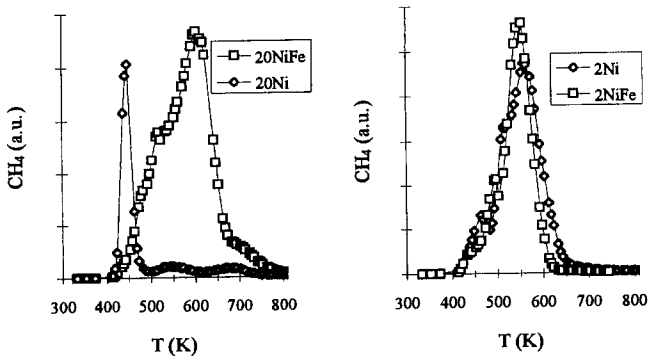

Fig. 6. TPH profiles of 20NiFe/TiO_2 and 20Ni/TiO_2 (left) and of 2NiFe/TiO_2 and 2Ni/TiO_2 (right) after 6 h of Fischer–Tropsch synthesis.

The TPH profiles of the low-loaded catalysts are almost identical. A small amount of α'-carbon and a large amount of α-carbon is present, whereas β-carbon is absent. Both catalysts produce higher hydrocarbons in Fischer–Tropsch synthesis and deactivate with time on stream. Obviously, for both properties at least α-carbon is necessary.

TPH profiles of the 2NiFe/TiO_2 and 20NiFe/TiO_2 catalysts are measured after 1 and 6 h of Fischer–Tropsch synthesis. The TPH profiles of 2NiFe/TiO_2 show that the amount of α'-carbon does not change with time on stream, whereas the amount of α-carbon increases significantly. So α-carbon may be responsible for the deactivation with time during the Fischer–Tropsch synthesis. The TPH profiles of 20NiFe/TiO_2 show more or less similar changes with time on stream, though the rise in α-carbon is smaller.

Furthermore, TPH profiles of 20NiFe/TiO_2 are measured immediately after 6 h of synthesis and after 6 h of synthesis and subsequently 1 h of treatment in a flow of hydrogen at 525 K. The TPH profile after the additional 1 h in hydrogen shows that all α'-carbon has disappeared and that part of the type α-carbon has been hydrogenated also. Obviously, these types of carbon are the active species in the Fischer–Tropsch synthesis at 525 K. After 1 h in a stream of hydrogen at 525 K β-carbon is still present, which is hydrogenated above about 670 K, demonstrating that this type of carbon is not active under Fischer–Tropsch conditions.

From combining the TPH experiments presented in fig. 6 and the Fischer–Tropsch results several types of carbon have been distinguished. Carbon which is hydrogenated below 500 K (α'-carbon) can be related to the formation of methane. These carbon species do not cause deactivation with time on stream. Furthermore, carbon which is hydrogenated between 500 and 650 K (α-carbon) is involved in the formation of higher hydrocarbons and its growing amount causes presumably deactivation. This α-carbon may be connected to the decrease of the magnetization during Fischer–Tropsch synthesis (fig. 5). Finally, carbon which is hydrogenated above 650 K (β-carbon). This type of carbon (presumably graphite) is not active in the Fischer–Tropsch synthesis and can, consequently, only contribute to the deactivation, explaining that the deactivation of the high-loaded catalyst is relatively larger than the deactivation of low-loaded catalysts.

3.6. A model for the nickel–iron on titania system

In fig. 7 a simple model for the catalysts is presented,

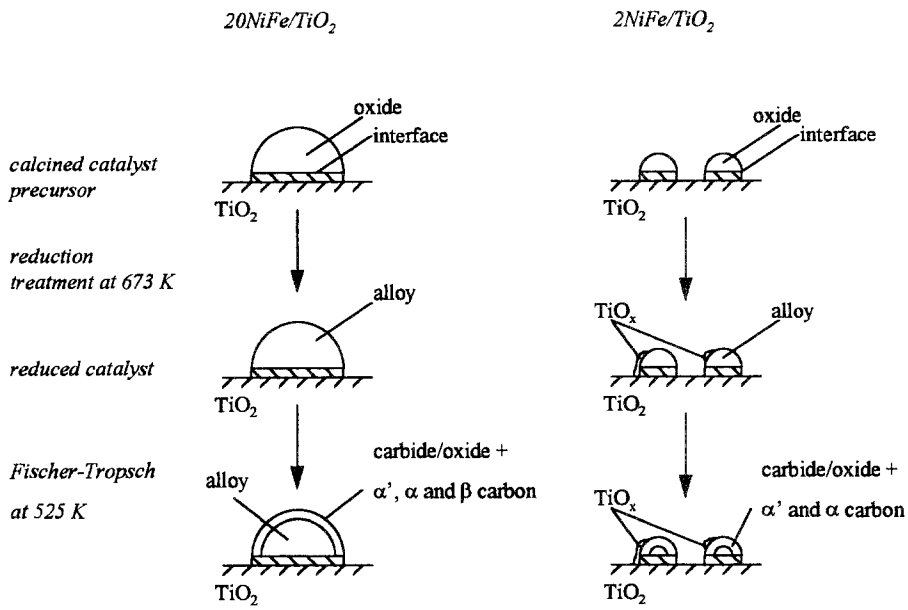

Fig. 7. A model for the nickel–iron on titania system.

which can describe all experimental results obtained with the measurements mentioned above.

The size of the alloy particles 20NiFe/TiO_2 is about three times that of the alloy particles of 2NiFe/TiO_2 (table 2). After preparation and calcination a mixed nickel–iron oxide phase is present in all nickel–iron catalysts [2,8]. Magnetic and Mössbauer experiments indicate that after reduction a nickel–iron alloy is present and also an oxidic interface, with at least Fe(II) between the titania support and the nickel–iron alloy. The thickness of this interfacial layer is probably independent of the metal loading. After reduction of 2NiFe/TiO_2 at 673 K probably TiO_x ($x < 2$) species are present on the surface of the alloy particles. This result was also found for titania-supported nickel catalysts [1,2,6].

The presence of TiO_x species on the surface of 2NiFe/TiO_2 will change the CO and hydrogen adsorption and dissociation properties of the alloy surface as compared to the alloy surface of 20NiFe/TiO_2. The CO dissociation is promoted by the presence of TiO_x, whereas the dissociation of hydrogen is decreased. This causes an increase in the ratio of dissociated CO to dissociated hydrogen on the alloy surfaces with increasing metal loading. Such can influence the effects which occur during Fischer–Tropsch synthesis.

Magnetic and Mössbauer experiments indicate formation of surface oxides and/or carbides during Fischer–Tropsch synthesis, whereas the bulk of the particle remains alloyed nickel–iron. TPH measurements show the existence of three types of carbon, which are hydrogenated at different temperatures. α'-carbon (400–500 K) involved in the formation of methane, α-carbon (500–650 K) involved in the production of higher hydrocarbons, while the deactivation of the catalysts is caused by α-carbon and β-carbon (> 650 K). β-carbon, most likely graphite, is only present on the high-loaded catalysts. The absence of β-carbon on low-loaded catalysts can be explained by the fact that graphite will not be formed on small metal particles but only on the larger alloy particles, which are present in the high-loaded catalysts [4].

During Fischer–Tropsch synthesis over 20NiFe/TiO_2 the nickel–iron alloy gives rise to the production of higher hydrocarbons. The increase in selectivity towards higher hydrocarbons of catalyst 2NiFe/TiO_2 is most likely caused by changes in the CO and H_2 dissociation properties induced by the presence of TiO_x species on the nickel–iron surface.

4. Conclusions

Low-loaded titania-supported nickel–iron catalysts are more selective towards higher hydrocarbons then high-loaded catalysts most likely due to the presence of TiO_x ($x < 2$) species on the surface of the active phase. These TiO_x species decrease the CO and H_2 chemisorption, but increase the dissociative adsorption of carbon monoxide of the catalyst.

Different types of carbon are involved in the formation of methane and higher hydrocarbons as well as in the deactivation of the catalysts. α'-carbon causes the formation of methane while α-carbon gives rise to the production of higher hydrocarbons. The deactivation of the catalysts is caused by α- as well as β-carbon.

Acknowledgement

The authors would like to thank Geert Mesland and

Djimmer de Blauw for part of the experimental work and André van der Horst and Leo Boellaard for part of the Mössbauer experiments.

References

[1] J. van de Loosdrecht, A.J. van Dillen, A.M. van der Kraan and J.W. Geus, J. Catal., submitted.
[2] J. van de Loosdrecht, PhD Thesis, Utrecht University, Utrecht, The Netherlands (1995).
[3] E. Iglesia, S.C. Reyes, R.J. Madon and S.L. Soled, Adv. Catal. 39 (1993) 221.
[4] F. van Looij, PhD Thesis, Utrecht University, Utrecht, The Netherlands (1994).
[5] S.J. Tauster, S.C. Fung and R.L. Garten, J. Am. Chem. Soc. 100 (1978) 170.
[6] S.J. Tauster, Acc. Chem. Res. 20 (1987) 389.
[7] G.B. Raupp and J.A. Dumesic, J. Phys. Chem. 88 (1984) 660.
[8] J. van de Loosdrecht, A.J. van Dillen, A.A. van der Horst, A.M. van der Kraan and J.W. Geus, Topics in Catal. 2 (1995) 29.
[9] P.W. Selwood, *Chemisorption and Magnetization* (Academic Press, New York, 1975).
[10] H.P.C.E. Kuipers, Solid State Ionics 16 (1985) 15.
[11] O.L.J. Gijzeman, XPS analysis of catalyst surfaces, unpublished.
[12] H.P. Klug and L.E. Alexander, *X-Ray Diffraction Procedures* (Wiley, New York, 1974).
[13] P. Scherrer, Gött. Nachr. 2 (1918) 98.
[14] S.J. Tauster and S.C. Fung, J. Catal. 55 (1978) 29.
[15] C.E. Johnson, M.S. Ridout and T.E. Cranshaw, Proc. Phys. Soc. 81 (1963) 1079.
[16] J.G. McCarty and H. Wise, J. Catal. 57 (1979) 406.